Aquaculture 575 (2023) 739778

Contents lists available at ScienceDirect

Aquaculture

journal homepage: www.elsevier.com/locate/aquaculture

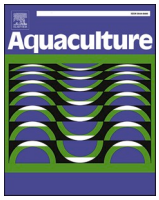

Integrated miRNA and mRNA analysis in gills of spotted sea bass reveals novel insights into the molecular regulatory mechanism of salinity acclimation

Lingyu Wang [a], Xiaoyan Zhang [b], Haishen Wen [a], Xin Qi [a], Donglei Sun [a], Xueqi Li [a], Jinku Li [a], Yuan Tian [a], Kaiqiang Zhang [a], Yun Li [a,*]

[a] Key Laboratory of Mariculture (Ocean University of China), Ministry of Education, Qingdao 266003, China
[b] School of Marine Science and Engineering, Qingdao Agricultural University, Qingdao 266109, China

ARTICLE INFO

Keywords:
Lateolabrax maculates
Osmoregulation
Gill histology
Transcriptome
miRNA-mRNA regulatory network

ABSTRACT

As a prominent abiotic factor, salinity affects fish growth, development, reproduction, and physiological activities severely. In the present study, we performed histological observations and miRNA-mRNA integrated transcriptomic analysis in the gill of spotted sea bass (*Lateolabrax maculatus*) under different salinity conditions. Histological investigation showed that the morphological indices (filament thickness, lamella thickness, lamella height, distance between lamella, lamella basal length) and the number of red blood and mucous cells were significantly different between FW and SW gills. A total of 1022 differentially expressed genes (DEGs) and 42 differentially expressed miRNAs (DEmiRs) have been identified among different salinity groups, generating 224 predicted miRNA-mRNA pairs that potentially associated with salinity acclimation. Protein-Protein Interaction networks revealed that 5 (*fbp1b*, *fbp2*, *gapdh*, *prkag2a* and *prkag3b*) and 7 (*zbtb16a*, *e2f5*, *brd4*, *brd3a*, *mef2ca*, *ncor1* and *ezh2*) hub genes may play important functions during FW and SW adaption, respectively. Notably, functional enrichment analysis suggested that DEGs and DEmiRs involved in glucose metabolism, signal transduction pathways, as well as hematopoiesis and vascular function maintaining associated molecules may be essential for osmoregulation in gills. Our findings will not only lay the basis for understanding the molecular mechanisms of salinity acclimation in euryhaline fishes, but also provide a list of molecular markers that can be used for improving fish salinity tolerance capabilities, and artificial breeding of salinity-tolerance strains for stenohaline species.

1. Introduction

Salinity represents a major abiotic factor that governs the activity, development and growth of fishes through complex biological interactions (Tian et al., 2019; Evans and Kultz, 2020; Kultz, 2015). When ionic and osmotic composition of external environment changes, fish typically undergo a series of physiological changes to maintain a stable internal body fluid homeostasis. However, dramatic fluctuations in water salinity may seriously influence their growth performance, survival rate, respiratory metabolism, reproductive development and muscle quality (Edwards and Marshall, 2012; Abou et al., 2016; Lisboa et al., 2015). Thus, exploring the key genes and regulatory factors involved in osmotic regulation and salinity acclimation will not only lay the crucial basis for understanding the molecular mechanism in response to salinity fluctuation, but also provide the molecular elements having potential to be used for improving fish salinity tolerance capabilities, and artificial breeding of salinity-tolerance strains (Edwards and Marshall, 2012; Yang et al., 2016).

For teleost fishes, gill, kidney and intestine are recognized as important organs for osmoregulation. Among them, the gill is one of the tissues directly expose to water for ion, water, oxygen exchange and is the predominant site that senses and responds to the external osmotic challenges (Lai et al., 2015). Recently, with the rapid development of high-throughput sequencing technology, a number of transcriptomic datasets generated from gill tissues in different salinity conditions have been reported from various species. For example, transcriptome analysis revealed that oxidative phosphorylation played essential roles in osmoregulation in gills of seawater acclimated guppy (*Poecilia*

* Corresponding author.
E-mail address: yunli0116@ouc.edu.cn (Y. Li).

https://doi.org/10.1016/j.aquaculture.2023.739778
Received 16 January 2023; Received in revised form 6 April 2023; Accepted 9 June 2023
Available online 10 June 2023
0044-8486/© 2023 Elsevier B.V. All rights reserved.

reticulata), and the downregulated expression of genes encoding V-ATPases and calreticulin had negative effect on the phagocytosis and immune response during this process (Chen et al., 2021). In the gill of Nile tilapia (*Oreochromis niloticus*), functional enrichment analyses of differentially expression genes (DEGs) indicated that mitochondrial energy metabolism, serine protease and immunity-related functions, and cytoskeleton / extracellular matrix organization were major molecular and cellular processes regulated by different salinities (Root et al., 2021). Moreover, gill transcriptomes in response to salinity changes have been widely investigated in fish species including goby (*Acanthogobius ommaturus*) (Sun et al., 2020), fathead minnows (*Pimephales promelas*) (Monroe et al., 2019), threespine stickleback (*Gasterosteus aculeatus*) (Gibbons et al., 2018) and marine medaka (*Oryzias melastigma*) (Liang et al., 2021). These studies identified several known and novel genes and pathways related to salinity regulation, which provide important resources for uncovering the molecular basis of osmoregulation in teleost fishes.

MicroRNAs (miRNA), a class of small non-coding RNAs (18–25 nucleotides), can regulate the expression of endogenous genes by binding to the 3′-untranslated regions (3'-UTR) of target mRNAs, leading to translational repression or RNA silencing (Obernosterer et al., 2006; Nilsen, 2007; Yang et al., 2013). As important gene expression regulators, miRNAs have function on the regulation of many biological processes, such as growth, organ development, signal transduction, abiotic stress response, cellular proliferation, and innate immune response (Obernosterer et al., 2006; Wienholds et al., 2005; Wienholds and Plasterk, 2005; Martin-Gomez et al., 2014; Xiao et al., 2014). The researches about the roles of miRNAs in response to acute salinity stress or during salinity acclimation have been conducted in some fish species, and several miRNAs and their target genes have been reported. For examples, miRNA-mRNA regulation pairs like osmotic stress transcription factor 1 (*ostf1*) -miR-429 (Yan et al., 2012a), insulin-like growth factor 1 (*igf1*)- miR-206 (Yan et al., 2013), heat shock protein 70 (*hsp70*)-miR-30c in Nile tilapia (Yan et al., 2012b) and sodium-hydrogen exchanger regulatory factor 1 (*nherf1*)-miR-8 in zebrafish (Flynt et al., 2009), have been demonstrated to play crucial roles in osmoregulation. By using the high-throughput sequencing platform and bioinformatic method, it was more easily to measure and compare expression levels of mRNA and miRNA within the same tissues or developmental stages simultaneously, thereby their potential regulatory relationships could be predicted and characterized through integrated analyses. Studies about the osmotic regulatory molecular mechanisms by using omics analysis methods have been performed on rainbow trout (*Oncorhynchus mykiss*; Yang et al., 2022) and Atlantic salmon (*Salmo salar*; Shwe et al., 2020; Pelis and McCormick, 2001), which suggested hormone biosynthesis, stress management, immune response, ion transport, and energy metabolism were closely associated with the salinity acclimation.

The spotted sea bass, *Lateolabrax maculatus*, as one of the most important commercial marine fishes in China (Liu et al., 2020; Zhang et al., 2022; Ren et al., 2022), created high economic values. The ability to maintain internal ionic and osmotic balance within a wide range of environmental salinity conditions (Zhang et al., 2017; Tian et al., 2020; Zhang et al., 2019) makes it an ideal model to investigate the osmoregulation mechanism. In the present study, we performed transcriptomic sequencing and integrated analysis of mRNAs and miRNAs in gills of spotted sea bass that had acclimated to sea water, fresh water and brackish water, respectively. Our findings identified potential key genes, miRNA and functional pathways responsible for osmoregulation, and uncover the interplaying among mRNA and miRNA during acclimation to different salinity environments. Understanding the molecular basis of salinity acclimation of spotted sea bass will not only provides theoretical guidance for its better rearing, but is also essential for the future improvement of salinity tolerance capability of stenohaline fish.

2. Materials and methods

2.1. Salinity acclimation experiment and sample preparation

The spotted sea bass juveniles were obtained from Shuangying Aquatic Seedling Co., Ltd. (Lijin, Shandong, China), and the water salinity was kept at 30 ‰. Prior to the experiment, 108 fish (average weight: 127.35 ± 15.31 g) were randomly transferred to nine 120 L cuboid tanks (n = 12 fish/tank) and temporarily reared for one week. During temporary rearing, each tank was filled with sea water under the following conditions: 25.3 ± 0.7 °C, dissolved oxygen 7.01 ± 0.45 mg/L, pH 7.8 ± 0.5 and salinity 30 ‰, with 14:10 h light-dark photoperiod. To maintain the above parameters approximately constant, one-third to one-half of the seawater was replaced each day. After that, by consistently adding fresh water, the salinities of three fish tanks were reduced gradually over 15 h (approximately 1–2 ‰ per hour) until they reached the 0 ‰ (fresh water group, FW). The salinities of another three fish tanks were adjusted to the 12 ‰ (brackish water group, BW) by a gradual decrease of 1–2 ‰ salinity per hour over 12 h. The salinities of the other three tanks were kept at 30 ‰ (sea water group, SW). Experiment was lasted for one month and fish were fed with commercial diet once daily. The experimental conditions were maintained by daily replacement of one-third to one-half of the prepared water with different salinity. After 30 days rearing, 6 fish per tank were treated with tricaine methane sulfonate (MS-222, 200 mg/L). The gill arch with gill filament were dissected and placed in the PBS solution to wash away any residual blood and mucus. After removing the excess PBS with absorbent gauze, parts of gill filament were collected immediately in liquid nitrogen and stored at −80 °C for RNA extraction, and the other parts were fixed with 4% paraformaldehyde solution for 24 h and maintained in 70% ethanol for histological observation. The RNA extraction and paraffin embedding were performed within one week after sampling. Total RNA and miRNA were isolated from gill tissues of spotted sea bass using TRIzol Reagent (Invitrogen, Carlsbad, USA) following the manufacturer's protocol, respectively. The quantity and integrity were examined with Bioanalyzer 2100 (Agilent, Santa Clara, USA) and RNA 6000 Nano LabChip Kit (Agilent, Santa Clara, USA). To improve the samples reproducibility without increasing the number of sequenced individuals, equal amounts (500 ng) total RNA from 6 individual fish in the same salinity tank were pooled as one sample, and 3 replicated samples were obtained from 18 individuals in each salinity treatment group (FW, BW, SW) for library preparation.

2.2. Histological observation of gills

Paraformaldehyde fixed gill samples collected from FW and SW groups were dehydrated with graded ethanol (70%, 80%, 95% and 100%), vitrification by xylene (xylene: ethanol absolute 1:1 and 100% xylene), embedded in paraffin and sectioned into 5 μm sections using a sliding microtome (LEICA-RM206). The paraffin-fixed sections were flattened when floated on the 40 °C warm water, then picked up by the glass slides and exsiccated in the oven at 37 °C for over 8 h. The exsiccated sections were dewaxed using xylene and graded ethanol (100%, 95%, 80%, 70% and 50%), and followed by tap water rinsing. The tissue was subsequently stained with haematoxylin and eosin (H&E) (Sabaliauskas et al., 2006). Then the sections were dehydrated with ethanol (95% and 100%) and xylene and sealed with neutral gum. The images were captured using OLYMPUS BX53 microscope.

2.3. RNA-seq and miRNA library construction and sequencing

A total of nine mRNA sequencing libraries (3 treatment groups × 3 replicated samples) were constructed from purified RNA of gill tissues in accordance with the protocol for the TruSeq RNA sample preparation Kits (Illumina, San Diego, USA). Then, the libraries were sequenced using an Illumina Novaseq™ 4000 platform (LC-BIO, Hangzhou, China)

to generate 150 bp paired-end (PE) reads. Raw sequences were deposited in the Short Read Archive of the National Center for Biotechnology Information (NCBI) with accession numbers of PRJNA515986.

For miRNA sequencing, the same gill samples as mRNA transcriptome sequencing were used and nine small RNA libraries were constructed using the TruSeq Small RNA Sample Prep Kits (Illumina, San Diego, USA) according to the manufacturer's protocol. Briefly, the 3′ and 5′ adapters were ligated to 3′ and 5′ ends of small RNA, respectively. Then the first-strand cDNA was synthesized and amplified by PCR. After that, the PCR products in the length range of 140–160 bp were further purified on 6% polyacrylamide Tris-borate-EDTA gel to complete the preparation of the miRNA library and then sequenced using the Illumina HiSeq2500 platform, generating 50 bp single-end (SE) read. All raw data for miRNA sequencing were available in the NCBI database with accession numbers of PRJNA550029.

2.4. Identification of differential expressed genes (DEGs)

The quality of mRNA sequencing data was evaluated by FastQC software (v0.11.9). After trimming adapter sequences, ambiguous nucleotides, filtering low-quality reads and short reads (length < 100 bp) using Cutadapt (v1.9), clean reads of FW, BW and SW groups were obtained for each RNA-seq library and were aligned to the reference genome of spotted sea bass (PRJNA408177) using HISAT2 (v2.0.4), while the designated gene location information was counted according to the genome annotation. The readscount for DEGs identification were obtained by using StringTie (v1.3.4d). DEGs among the three comparisons (FW vs. SW, FW vs. BW and SW vs. BW) were identified by DESeq2 package (v1.34.0), with the significant threshold was settled as $|\log2\text{-foldchange}| \geq 1$ and $p < 0.05$. Meanwhile, the gene expression level was measured as fragments per kilobase of transcript per million fragments mapped (FPKM) for hierarchical cluster analysis by using StringTie and extract by Ballgown package (v2.26.0).

2.5. Protein-protein interaction (PPI) networks construction and hub gene identification

PPI networks were constructed using online software STRING (https://string-db.org/), and visualized by Cytoscape (v3.8.2). Hub genes were selected by Molecular Complex Detection (MCODE) plugin (v2.0.2), with the following parameters: score > 4.5, degree cutoff $= 2$, node score cutoff $= 0.2$, k-core $=2$, and max depth from seed $= 100$. Function enrichment for the hub genes was done by using CluGO plugin (v2.5.9) under the criterion of kappa score $= 0.4$. The related biological process terms and KEGG pathways were clustered in the significant groups.

2.6. miRNA identification and expression profiling

The small RNA raw reads were filtered using the ACGT101-miR (v4.2; LC Sciences, Houston, USA), to remove the adapter dimers, junk, low complexity, common RNA families (rRNA, tRNA, snRNA and snoRNA), and repeats. The remaining clean sequences with length of 18–26 nucleotide were mapped to mature miRNAs and pre-miRNAs of vertebrata species (including teleostei, sauria and mammalia; Table S1) in miRBase 22.0 by BLAST to identify conserved known miRNAs. The unmapped sequences were aligned with the reference genome of spotted sea bass, and the hairpin RNA structures containing sequences were predicated from the flanking 80 nt sequences using RNAfold software (http://rna.tbi.univie.ac. at/cgi-bin/RNAfold.cgi) to detect novel miRNAs. Data normalization was performed by ACGT101-miR (v4.2) software followed the procedures as described in a previous study (Zhang et al., 2013; Li et al., 2016). The differentially expressed miRNAs (DEmiRs) between samples were identified and p-value was estimated by selectively using t-test (http://en.wikipedia.org/wiki/Student's_t-test). The significance threshold was set as 0.05.

2.7. Integrated analysis of mRNA and miRNA data

The prediction of target genes of miRNAs was performed using two computational target prediction software including TargetScan v5.0 (TargetScan_score $\geq$ 50) and miRanda v3.3a (miranda_Energy $\langle -10$). The overlaps of these two software were retained as the ultimate target genes of DEmiRs. Although the relationship between miRNA and mRNA is not completely negative, in this research, we only focus on the pairs displayed negative correlation pattern. Cytoscape (v3.8.2) software was used to construct miRNA-mRNA interaction network of the screened pairs.

2.8. Real-time quantitative PCR validation for mRNA and miRNA

Quantitative real-time PCR (qPCR) was used to detect the expression levels of 6 DEmiRs and their 6 target DEGs to validate our bioinformatic analysis results. In order to confirm the identified salinity-responsive genes and miRNA were not aroused by experimental errors or fish individual differences, we conducted a separate salinity acclimation experiment to test the expression levels. For this time, 30 spotted sea bass (average weight: 812 ± 25.71 g) were acclimated in six 400 L plastic drums for one week with the same water conditions as the above experiment. Subsequently, the salinity of three drums were gradually decreased to 0 ‰ over 12 h (FW group), and the other three drums were kept at 30 ‰ (SW). After 14 days, gill tissues of 3 fish individuals each drum were collected, and their total RNAs and small RNAs were extract by TRIzol® reagent (Invitrogen, Carlsbad, USA) and MiPure Cell/Tissue miRNA Kit (Vazyme, Nanjing, China), respectively.

Genomic DNA was removed from total RNA and reverse-transcribed into cDNA using the PrimeScript™ RT kit (TaKaRa, Shiga, Japan) to quantify mRNA. For small RNAs, genomic DNA was discarded using DNase I (TaKaRa, Shiga, Japan) and reverse-transcribed into cDNA using the Mir-X™ miRNA First-Strand Synthesis kit (TaKaRa, Shiga, Japan). miRNAs were poly(A)-tailed using poly(A) polymerase, and then copied using a modified oligo(dT) primer and reverse transcriptase. The universal mRQ 3' Primer supplied with the kit was used as the qPCR reverse primer. The gene-specific primers and miRNA-specific forward primers were designed based on the gene and miRNA sequence using the Primer5 software and listed in Table S2. The 10 μL reaction mixture consisted of 2 μL template cDNA, 0.2 μL of each primer, 5 μL of SYBR qPCR Mix (2×) and 2.6 μL of nuclease-free water. PCR amplification was performed as that incubated in a 96-well optical plate at 95 °C for 5 s, followed by 40 cycles of 95 °C for 5 s and 56 °C for 30 s with a final dissociation curve to verify the specificity of the amplified products. qPCR was performed using the StepOne Plus Real-Time PCR system (Applied Biosystems) and $2^{-\Delta\Delta CT}$ method was used to analysis the expression level of genes. 18S ribosomal RNA and U6 snRNA (forward primer: TGGAACGCTTCACGAATTTGCG; reverse primer: GGAACGATACAGAGAAGATTAGC) was used as the internal controls for mRNA and miRNA, respectively. The correlation coefficient between the fold changes in RNA-Seq and qPCR was determined by SPSS21.0, and one-way ANOVA followed by Duncan's multiple range tests and differences were accepted as statistically significance when $P < 0.05$.

3. Results

3.1. Histological structure of gills in different salinities

Histological sections showed that there were significant morphological differences in the gills of spotted sea bass after acclimation to different salinity environments (Fig. 1). Compared with the fish individuals in SW group, the number of mucous cells (MC) on the gill lamella (also named as secondary lamellas) were significantly increased (1.29 ± 1.09 to 2.42 ± 1.49 each lamellas), and the number of red blood cells (BC) was decreased after adapted to FW condition (24.54 ± 3.44 change to 19.54 ± 2.86 each lamellas). Meanwhile, ionocytes (also

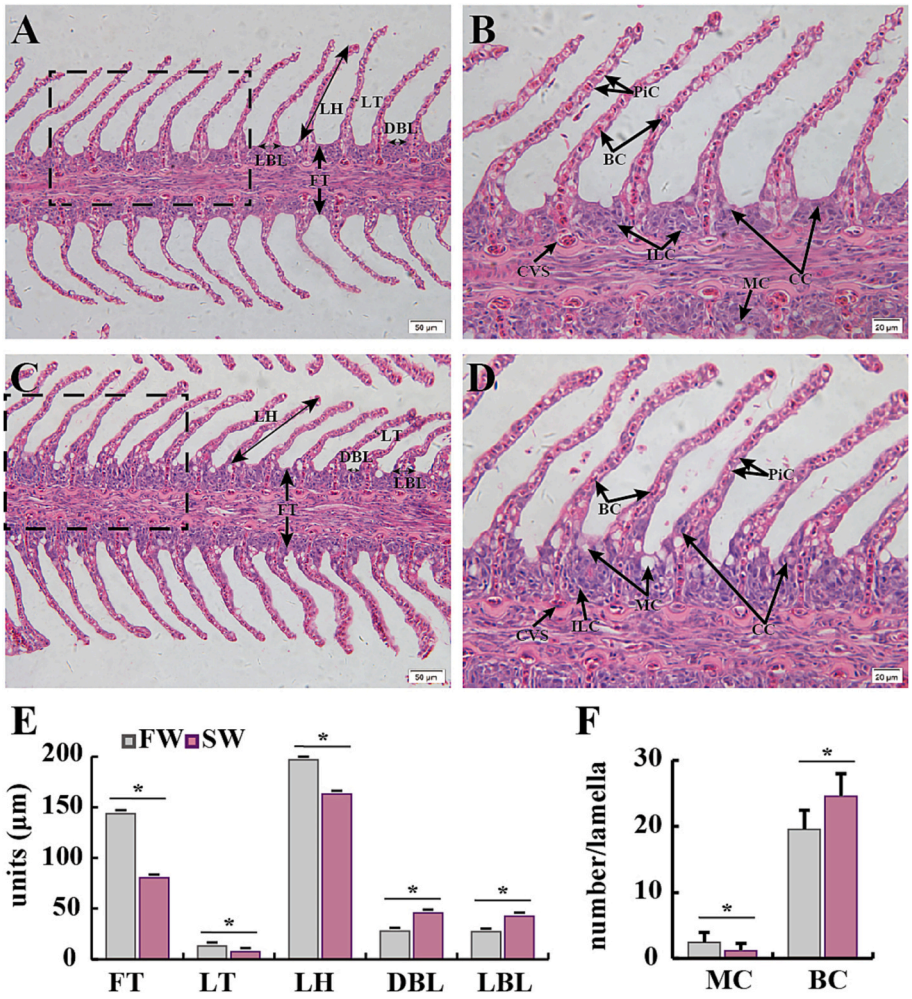

Fig. 1. Histological observation of gills in spotted sea bass at SW and FW groups. A. Histological image of the gill in SW-acclimated spotted sea bass. B. The enlarged view of the dashed boxes in Fig. 1A. C. Histological image of the gill in FW-acclimated spotted sea bass. ILC, interlamellar cells; CC, chloride cells (ionocytes); PiC, pillar cells; MC, mucous cells; CVS, central venous sinus; BC, red blood cells. D. The enlarged view of the dashed boxes in Fig. 1C. E. Morphological indices of gills at SW and FW groups. FT, Filament thickness; LT, Lamella thickness; LH, Lamella height; DBL, Distance between lamella; LBL, lamella basal length. Data are presented as mean ± SEM for each group tested. Different letters represented significant differences between groups($P < 0.05$, $n = 30$). (For interpretation of the references to colour in this figure legend, the reader is referred to the web version of this article.)

named as chloride cells, CC) were distributed in different positions on the gill lamella when adapted to different salinities. In SW group, the ionocytes were located mainly in the interlamellar region, while in FW group, they also appeared on the lateral surfaces of the gill lamellas (Fig. 1A-D). In addition, the filament thickness (FT), lamella thickness (LT) and the lamella height (LH) in FW group (143.62 ± 18.85 um, 13.17 ± 0.65 um, and 196.67 ± 5.93 um, respectively) showed significantly increase compared to those in SW group (80.44 ± 1.74 um, 7.5 ± 0.32 um, and 162.89 ± 3.66 um, respectively). Meanwhile, the distance between lamella (DBL) and the lamella basal length (LBL) were significantly decreased in FW group (27.59 ± 0.95 um, and 27.08 ± 0.98 um, respectively) compared with SW group (45.65 ± 0.99 um, and 42.55 ± 0.61 um, respectively) (Fig. 1E).

3.2. Statistics for RNA-Seq data

RNA-Seq was carried out on gill samples from fish individuals of three different salinity groups (FW, BW and SW groups). A total of 409 million raw reads were obtained from the nine gill samples. After preprocessing and removal of low-quality sequences, totally 400,298,802 clean reads were generated (Table S3), with 124 million, 139 million and 138 million qualified clean reads for the FW, BW, and SW groups, respectively. The mapping ratio of clean reads to the spotted sea bass genome varied from 87.41% to 89.55% for the 9 samples (Table S3).

3.3. Identification of DEGs among different salinity groups

To evaluate the molecular response of gills to different salinities in spotted sea bass, pairwise comparison analysis of gene expression levels was performed for three groups including FW vs. SW, FW vs. BW and SW vs. BW, respectively. As a result, a total of 1022 DEGs were identified. 266 genes showed significantly differential expressed in the FW group relative to BW group, of which 178 genes were up-regulated and 88 genes showed down-regulated. A total of 327 genes were differentially expressed in the SW group in comparison with BW group, including 214 up-regulated genes and 113 down-regulated genes. Additionally, totally 715 DEGs were found in the SW group compared to the FW group, with 503 up-regulated and 212 down-regulated genes (Fig. 2A).

According to the expression patterns among different salinity groups, these DEGs were further classified into three clusters (I-III, Fig. 2B) by hierarchical cluster analysis with complete linkage method. It represented that within each cluster, DEGs exhibited similar expression pattern, but it was markedly different from the other two clusters. As results showed, 329 DEGs were categorized to Cluster I, which had higher expression levels in FW than those in BW and SW; Cluster II harbored 68 DEGs, exhibiting higher expression levels in BW compared to FW and SW; Cluster III contained 625 DEGs, the expressions of which in SW were significantly higher than those of FW and BW (Fig. 2B). Therefore, DEGs in Cluster I and III were induced significantly in FW and SW adaptions, respectively, which were considered to play essential roles in salinity acclimation of spotted sea bass.

3.4. Functional enrichment analysis of DEGs

To determine the potential biological functions of DEGs involved in salinity acclimation, GO and KEGG enrichment analysis were performed

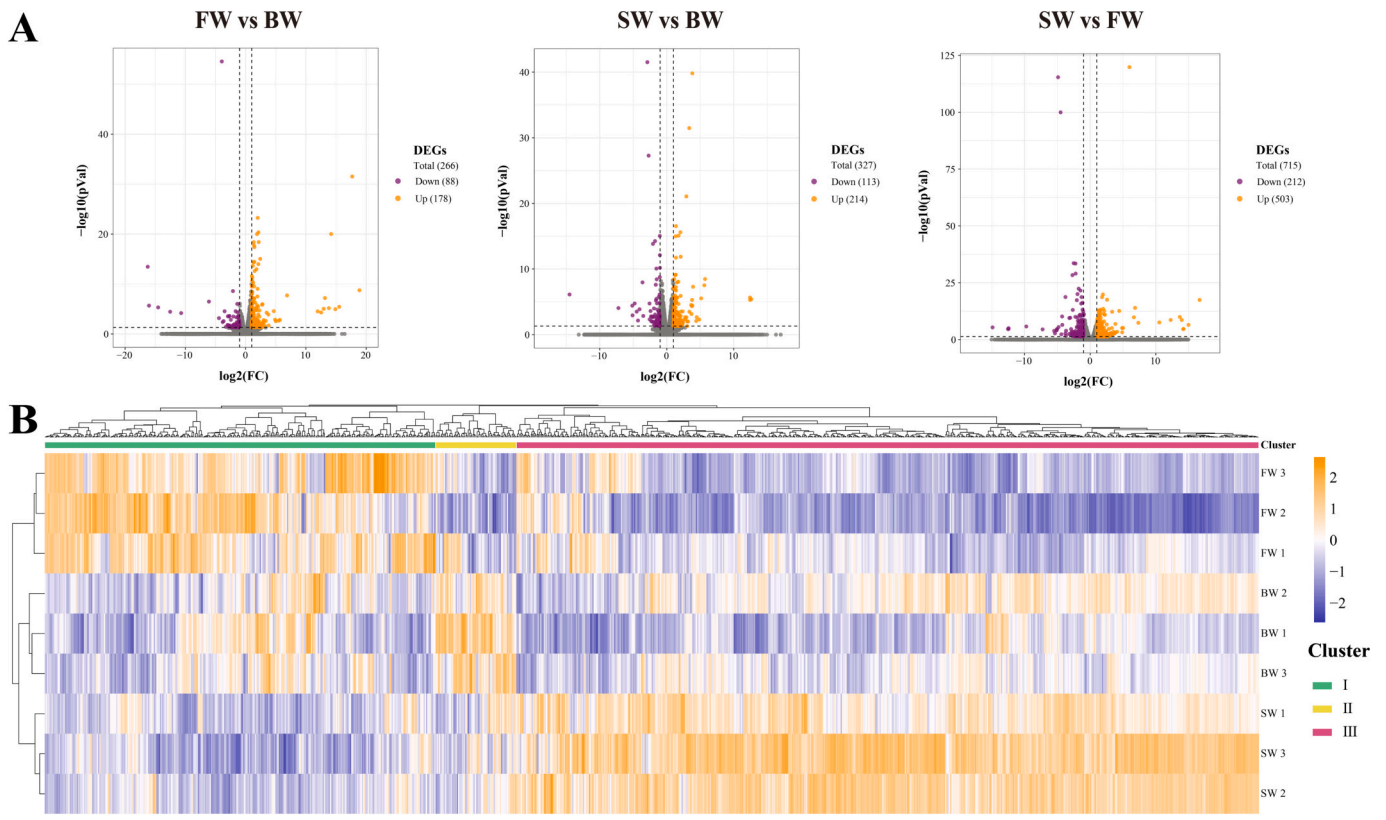

Fig. 2. Expression profiles for differential expressed genes (DEGs) among different salinity groups. A. Volcano plots displayed the expression profiles of the DEGs in pairwise comparisons (FW vs BW, SW vs BW and FW vs SW, respectively); B. Hierarchical cluster analysis of DEGs. Higher expression level was showed in orange, and lower expression level was indicated in blue. (For interpretation of the references to colour in this figure legend, the reader is referred to the web version of this article.)

for DEGs belonging to Cluster I and III, respectively. As shown in Fig. 3A, DEGs in Cluster I were primarily enriched in cellular junction and ion transport related GO terms, such as "bicellular tight junction assembly" and "potassium ion import across plasma membrane". Meanwhile, KEGG enrichment analysis revealed that DEGs in Cluster I were significantly enriched in metabolic pathways, the most of which belonged to amino acid and carbohydrate metabolism related pathways (Fig. 3B).

Meantime, DEGs in Cluster III that were induced significantly in SW condition were concentrated in transcription regulation associated GO terms (Fig. 3C). KEGG enrichment analysis indicated that a number of signal transduction associated pathways and metabolism related pathway like "phosphatidylinositol signaling system" and "Glycosphingolipid biosynthesis" were concentrated in Cluster III. In addition, pathway like "C-type lectin receptor signaling pathway" and "Vascular smooth muscle contraction" involved in immune and circulatory systems were also enriched in Cluster III (Fig. 3D).

3.5. Protein-protein interaction (PPI) networks

The network for DEGs within Cluster I was built by 157 nodes and 220 edges, and 5 hub genes, including fructose 1,6-bisphosphatase 1b (*fbp1b*), fructose 1,6-bisphosphatase 2 (*fbp2*), glyceraldehyde-3-phosphate dehydrogenase (*gapdh*), protein kinase amp-activated non-catalytic subunit gamma 2a (*prkag2a*) and protein kinase amp-activated non-catalytic subunit gamma 3b (*prkag3b*), were identified by using MCODE plugin (Fig. 4A). Meanwhile the networks for Cluster III consisted of 400 nodes and 868 edges, and 7 genes, including zinc finger and BTB domain containing 16a (*zbtb16a*), E2F transcription factor 5 (*e2f5*), bromodomain containing 4 (*brd4*), bromodomain containing 3a (*brd3a*), myocyte enhancer factor 2ca (*mef2ca*), nuclear receptor corepressor 1 (*ncor1*) and enhancer of zeste 2 polycomb repressive complex 2 subunit (*ezh2*), were recognized as hub genes (Fig. 4B). GO annotation results showed that the top processes by which hub genes of Cluster I significantly enriched were glucose metabolic process and phosphorus metabolic process (Fig. 4C). Meanwhile, cell proliferation and differentiation related processes such as thrombocyte differentiation were significantly enriched by hub genes in Cluster III (Fig. 4D). For KEGG analysis, results indicated that hub genes in Cluster I were concentrated in "Insulin signaling pathway", "Glycolysis/Gluconeogenesis" and "Adipocytokine signaling pathway", while Cluster III were concentrated in "MAPK signaling pathway", "Lysine degradation" and "Cellular senescence" (Fig. 4E, F).

3.6. Characteristics of identified miRNAs

Nine miRNA libraries for gill tissues of three salinity groups, which were consistent with RNA-seq samples, were constructed and generated a total of 98,128,742 raw reads. After removing low-quality reads, empty adaptor sequences and sequences shorter than 18 nt and longer than 32 nt, a total of 73,892,305 valid reads were obtained (Table S4). 24,320,410, 25,598,497, 23,973,398 clean reads were collected from FW, BW, SW groups, respectively. 80.69% of the total mappable reads were distributed in the length of 21–23 nt, and the ratio of 22 nt read was the highest (Table S5). A total of 844 mature miRNAs were identified in gills of spotted sea bass, including 664 known miRNAs and 180 novel miRNAs (Table S6). Among them, 747 mature miRNAs were mapped to 664 predicted pre-miRNAs on the reference genome.

3.7. DEmiRs among different salinity groups

The expression levels of miRNAs were compared in gills of spotted sea bass among different salinity groups. As shown in Fig. 5, in the FW

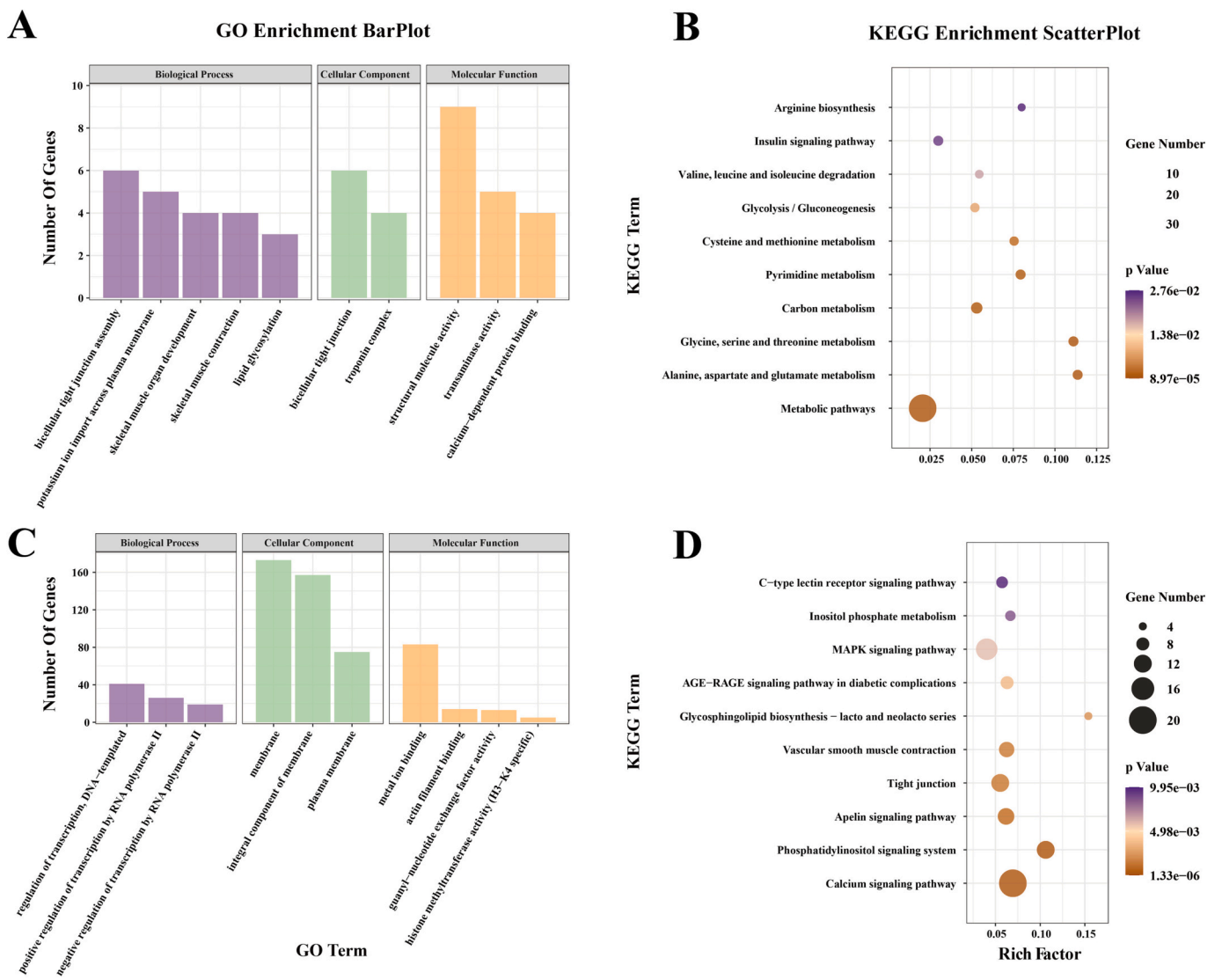

Fig. 3. Functional enrichment of DEGs among different salinity groups. A. Histogram of GO classifications for DEGs in Cluster I; B. KEGG enrichment analysis for DEGs in Cluster I; C. Histogram of GO classifications for DEGs in Cluster III; D. KEGG enrichment analysis for DEGs in Cluster III.

vs. BW comparison group, a total of 42 miRNAs showing significantly differential expression profiles were identified as DEmiRs, of which 19 DEmiRs were up-regulated in FW group and 23 miRNAs showed down-regulation. A total of 32 DEmiRs were identified within the SW vs. BW comparison group, including 18 up-regulated miRNAs by SW and 14 down-regulated miRNAs. Totally 38 DEmiRs were found between the SW vs. FW group with 21 up-regulated miRNAs and 17 down-regulated miRNAs (Fig. 5).

3.8. Regulatory network of DEmiRs and target DEGs

Candidate target genes of DEmiRs were predicted by TargetScan and miRanda. In combination with the analysis results of mRNA expression profiles, a total of 182 putative miRNA-mRNA negative correlation pairs (include 28 DEmiRs and 112 DEGs) were identified (Table S7), which may play important functions in gills of spotted sea bass during salinity adaption. To investigate the distribution of DEmiRs derived precursor miRNAs (pre-miRNAs) and their target DEGs in the reference genome of spotted sea bass, a circos plot were constructed (Fig. 6). The density of expressed miRNAs in gills was calculated in each bin (0.5 Mb) on chromosome (Chr), which was approximately 1 miRNA/ Mb. The density of DEmiRs was calculated in each 5 Mb on Chr. The average DEmiRs density in the genome was approximately 0.2 / Mb. Notably, Chr 2 and Chr 11 harbored the highest DEmiRs density across the genome, which were considered as DEmiRs hot bins (density > 1/Mb) (Fig. 6).

In addition, the potential miRNA-mRNA regulatory network was constructed by Cytoscape. Integrated analysis indicated that 39 DEGs in Cluster I were targeted by 13 DEmiRs, generating 85 miRNA-mRNA pairs, and 74 DEGs belonging to Cluster III were considered as the target genes of 16 DEmiRs, producing 139 miRNA-mRNA pairs (Fig. 7A). Subsequently, KEGG analysis showed that DEGs in Cluster I potentially regulated by DEmiRs were significantly enriched in “pentose phosphate pathway” and “histidine metabolism”. Meanwhile, the DEGs in Cluster III targeted by DEmiRs were concentrated in “C-type lectin receptor signaling pathway”, “phosphatidylinositol signaling system” and “ErbB signaling pathway” (Fig. 7B).

3.9. Overview of the key miRNA, mRNA, and functional pathways potentially involved in salinity acclimation

Based on above bioinformatic analysis about expression profiles of mRNA and miRNA, the predicted regulatory relationship among miRNA and their target genes, the functional enrichment results, in combination with manual literature searches, we summarized and drew the putative

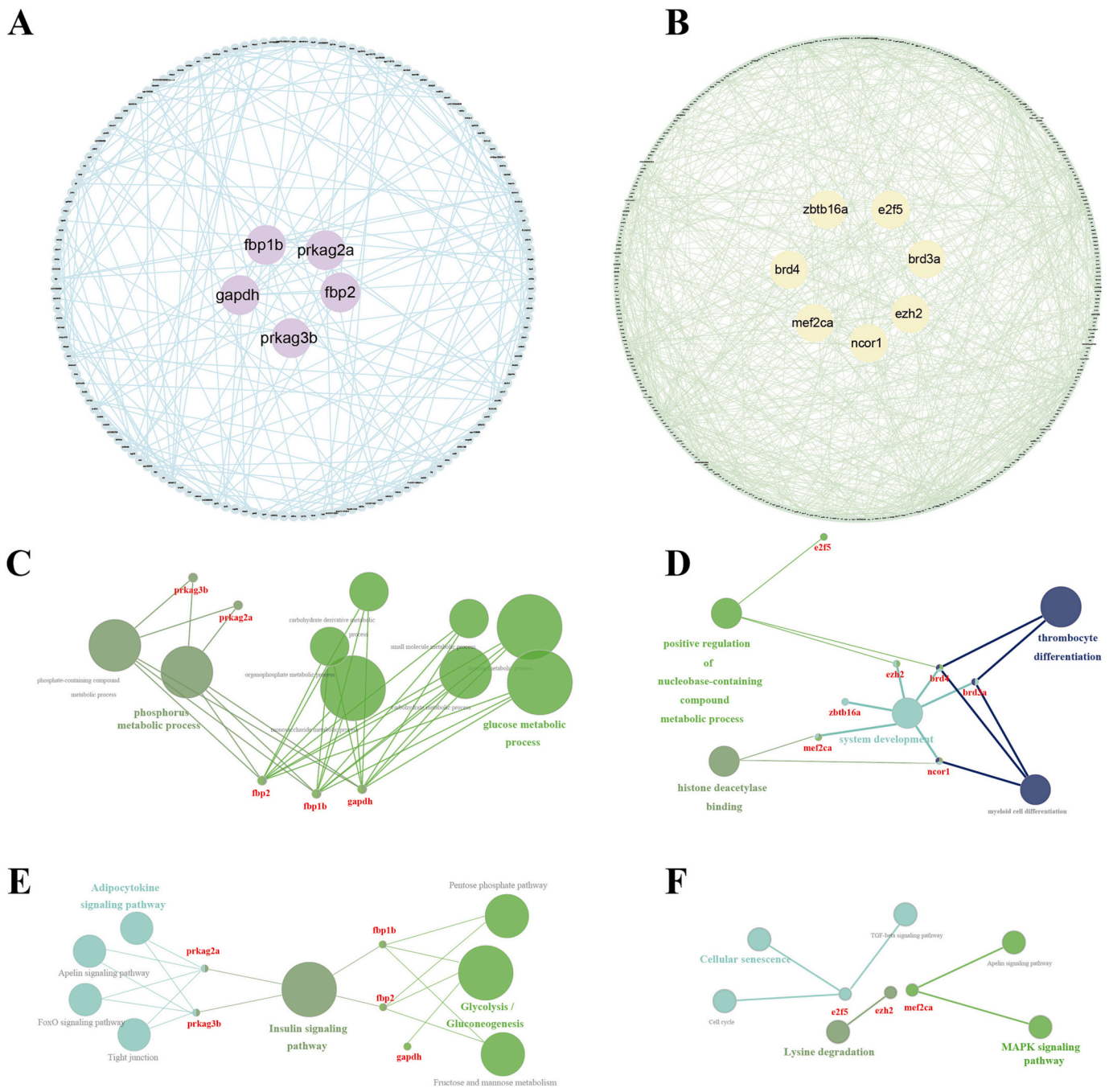

Fig. 4. PPI network construction and functional enrichment analysis for hub genes. A. The PPI network of DEGs in Cluster I; B. The PPI network of DEGs in Cluster III. The nodes represent proteins and edges represent interactions between proteins. Hub genes of Cluster I and Cluster III were filled with purple and yellow, respectively. C. Hub genes enriched biological processes by GO annotation of Cluster I; D. Hub genes enriched biological processes by GO annotation of Cluster III. E. Hub genes enriched KEGG pathways of Cluster I and; F. Hub genes enriched KEGG pathways of Cluster III. (For interpretation of the references to colour in this figure legend, the reader is referred to the web version of this article.)

schematic diagram presenting the master genes, miRNA and pathways engaged in gills of spotted sea bass during salinity acclimation (Fig. 8). Overall, during FW acclimation, four pathways were recognized to possess key regulators: 1) Glycolysis / Gluconeogenesis pathway: harbored *fbp1b*, *fbp2* (targeted by lma-miR-200b), and *gapdh*, which were also identified as hub genes in Cluster I; 2) Insulin signaling pathway: *fbp1b*, *fbp2*, *prkag2a* and *prkag3b* as the hub genes of Cluster I were included; 3) Pentose phosphate pathway: *fbp1b* and *fbp2* were also engaged in this pathway; and 4) Histidine metabolism pathway: lma-miR-203b-3p and its target gene uroc1 were recognized. On the contrary, when adapted to SW condition, main factors identified in our study concentrated in four processes: 1) Phosphatidylinositol signaling system pathway: *pik3ca* (targeted by lma-miR-727b) and *dgkh* (targeted by lma-miR-9a-3p), were identified; 2) ErbB signaling pathway: 3 DEmiRs (lma-miR-30c, lma-miR-9a-3p, lma-miR-210) participated in this process by targeting to *cblb*; 3) MAPK signaling pathway: one hub gene of Cluster III, *mef2ca*, and its regulatory miRNAs (lma-miR-101a-5p, lma-let-7i-3p and PC-5p-26548_93), were identified; 4) Cell cycle: *e2f5*, encoding transcription factor which play essential function in the control of cell cycle was recognized (Fig. 8A).

Moreover, it was worth noting that a number of hub genes in Cluster III and DEmiRs, which were considered playing essential functions

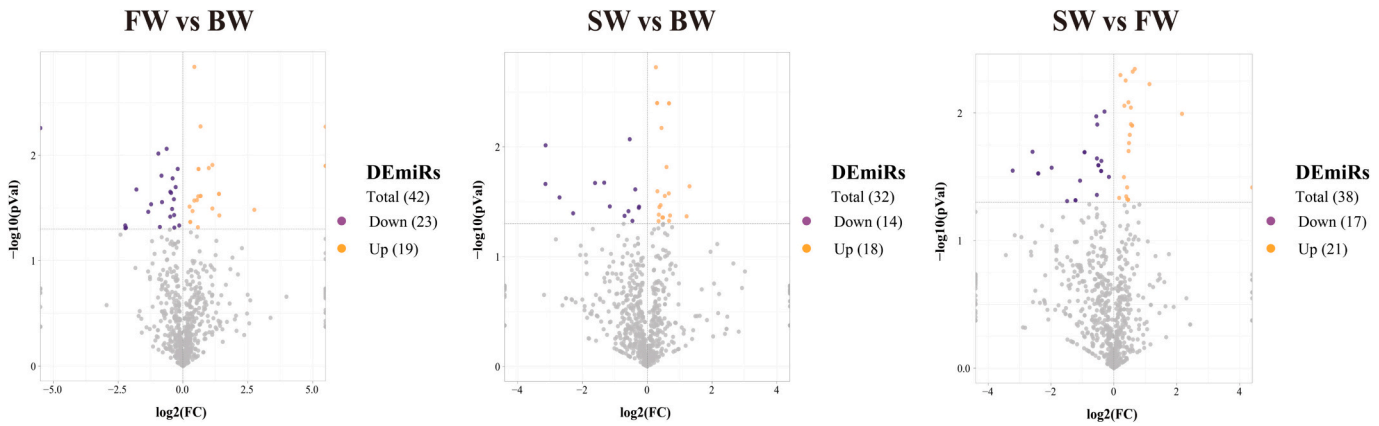

Fig. 5. The number of up/down-regulated differential expressed miRNAs (DEmiRs) in each comparison group (FW vs BW, SW vs BW and FW vs SW, respectively).

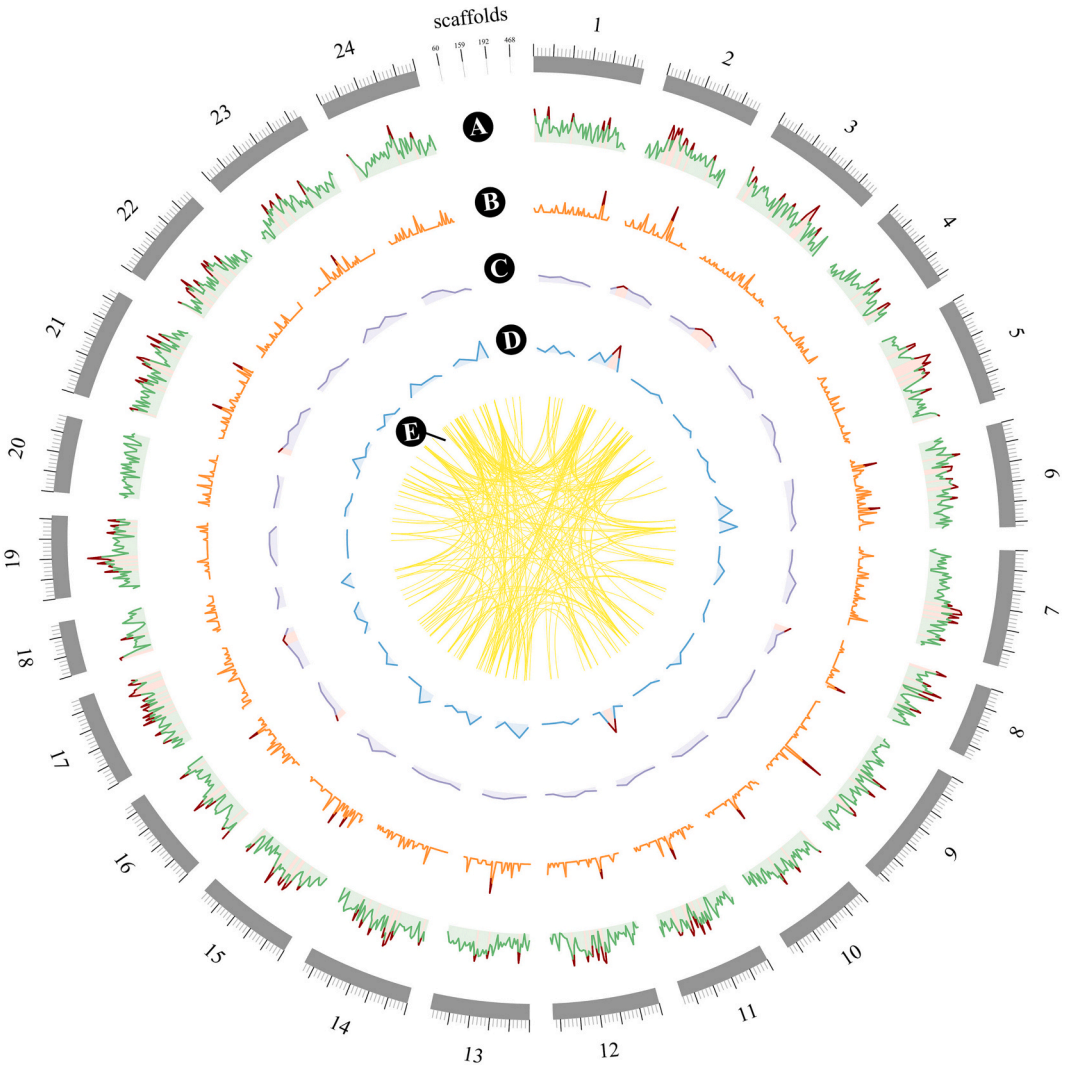

Fig. 6. Distribution of genes and precursor miRNAs (pre-miRNAs) in the reference genome of spotted sea bass. A. The distribution and density of gill expressed genes within a 0.5 Mb bin. B. The distribution and density of gill expressed miRNAs within a 0.5 Mb bin. C. The distribution and density of DEGs within a 5 Mb bin. D. The distribution and density of DEmiRs within a 5 Mb bin. E. The potential regulatory relationships between DEmiRs and their target DEGs. Hot bins (genes density > 60 / Mb; DEGs density > 3 / Mb; miRNAs >10 / Mb; DEmiRs density > 1 / Mb, respectively) were marked with red dots. (For interpretation of the references to colour in this figure legend, the reader is referred to the web version of this article.)

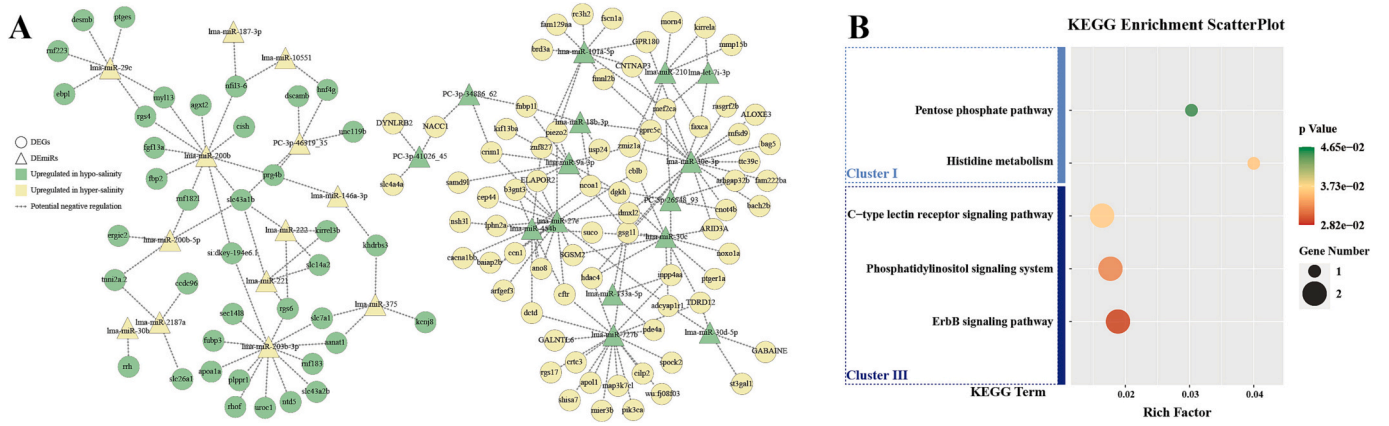

Fig. 7. Predicted miRNA-mRNA regulatory networks and their functional enrichment analysis in salinity acclimation. A. miRNA-mRNA regulatory networks potentially involved in salinity adaption. B. KEGG enrichment analysis of target DEGs in Cluster I and III.

during SW adaption, were identified as directly or indirectly related to the vascular events, which included but not limited to: 1) hematopoiesis associated elements including *brd3a*, *brd4*, *dgkh*, *cblb*, *zbtb16* and lma-miR-9a-3p, lma-miR-30c, lma-miR-210, lma-miR-101a-5p; 2) vascular function maintaining related regulators such as *mef2ca*, *pik3ca*, *ezh2*, *e2f5*, and lma-miR-101a-5p, lma-miR-727b, let-7i-3p. The detailed discussion regarding their potential biological functions in salinity acclimation were described in the Discussion section.

3.10. Validation of DEGs and DEmiRs by qPCR

To validate our bioinformatic analysis results, 6 DEmiRs (lma-miR-181c-5p, lma-miR-29c, lma-miR-23a-3p, lma-miR-2188, lma-miR-727b, lma-miR-200a and lma-miR-30e-3p) and 6 DEGs (*atp1b1b*, *zg16*, *il8*, *ptges*, *muc4*, *ccl20a.4*) from the screened miRNA-mRNA pairs were selected for qPCR analysis (Fig. 9). The results showed that the expression trends of those genes in qPCR were keep consistent with the RNA-Seq data.

4. Discussion

As essential regulators of gene expression, miRNAs are highly conserved and exert their influence by targeting mRNAs selectively (Nilsen, 2007; Flynt et al., 2009). MiRNAs regulation has been researched extensively during the past years (Pu et al., 2019), which showed that miRNA could regulate multiple target mRNAs, and vice versa, mRNA could be regulated by more than one miRNA (Wu et al., 2017). In this study, we provided a comprehensive annotation and analysis of parallel mRNA and miRNA expression in spotted sea bass exposed to different salinities, and obtained a number of salinity-responsive hub genes, pathways and miRNA-mRNA regulatory pairs, which help us to decipher the molecular mechanisms of salinity acclimation in euryhaline fishes. The consistency of transcriptome data and qPCR validation results, indicated the reliability and accuracy of the high throughput sequencing and data analysis.

According to the mRNA expression patterns in gills of spotted sea bass, DEGs of different salinity groups were divided into three clusters. Among them, genes in Cluster I and III displayed the higher expression levels in FW and SW group, respectively (Fig. 2), which attract more attention. Functional enrichment analysis showed that metabolism processes, especially amino acid and glucose metabolism related pathways were enriched in FW group. Previous studies have reported that the energy consumption for osmoregulation in FW is significantly more than it in SW environment (Ricardo and Peter, 1987), therefore, these activated metabolism processes may be required to meet the energy demand during hypo-salinity acclimation. The enhanced amino acid metabolism might be because that amino acids (such as taurine, glycine and L-serine) have been demonstrated to play important roles as osmolytes for FW acclimation in Senegalese sole (*Solea senegalensis*), whiteleg shrimp (*Litopenaeus vannamei*) and hard clam (*Meretrix lusoria*) (Aragao et al., 2010; Shinji et al., 2012; Lin et al., 2021).

Meantime, glucose metabolism may also be crucial for the acclimation to hypo-salinity environment in gills, which was indicated by PPI analysis results that *gapdh*, *fbp1* and *fbp2* encoding the rate-limiting enzymes in the glucose metabolism were recognized as hub genes in the network of FW group (Fig. 8A). Gapdh was reported as the key enzyme in the glycolytic pathway and catalyzed the conversion of glyceraldehyde-3-phosphate (G3P) to 1,3-biphosphoglycerate (1,3-P2G) in the presence of NAD^+ and inorganic phosphate to produce ATP (Douros et al., 2018; Nicholls et al., 2012). Meanwhile, the Fbp1 and Fbp2 were rate-limiting enzymes that catalyze the hydrolysis of fructose-1,6-bisphosphate to fructose-6-phosphate and inorganic phosphate (Sternisha and Miller, 2019; Park et al., 2020; Jiang et al., 2020). In our present study, down-regulation of lma-miR-200b during FW acclimation may up-regulate the expression of *fbp2* to enhance the glucose synthesis. Moreover, glucose is generally considered to be the main source of cell energy, and a major provider of carbon skeletons for cell growth and survival (Rajas et al., 2019). Therefore, higher activity of glucose metabolism could explain the higher growth rate in FW acclimated spotted sea bass, to a certain extent. In addition, *prkag2a* and *prkag3b* were also identified as hub genes in FW group, although their functions in osmoregulation have not been reported. However, both genes were involved in metabolism of phosphorus (Chaves Hernández, 2014), which is necessary to maintain the acid-base balance and carbohydrate metabolism. These results indicated that carbohydrate metabolism, especially glucose metabolic process was more active and important in gills under the FW conditions.

Fish have the ability to sense the osmolality of their environment and to transduce the sensory stimulus to signaling pathways that trigger many specific changes (Kultz, 2015). Correspondingly, for DEGs highly expressed in SW acclimation group, signal transduction pathways were significantly enriched (Fig. 3), especially MAPK signaling pathway, phosphatidylinositol signaling system and ErbB signaling pathway were identified as the potential key pathways (Fig. 8A). Similar discoveries have been made in several studies of teleost species, such as the marbled eel (*Anguilla marmorata*) (Cao et al., 2021) and rainbow trout (Zhou et al., 2022), in which signaling pathways including MAPK and Calcium signaling pathways were significantly enhanced after hyper-salinity acclimation.

Beyond that, a number of master genes and miRNAs were also significantly associated with the vascular system, which drives tissue convection of water, ions, respiratory gases, nutrients, waste products

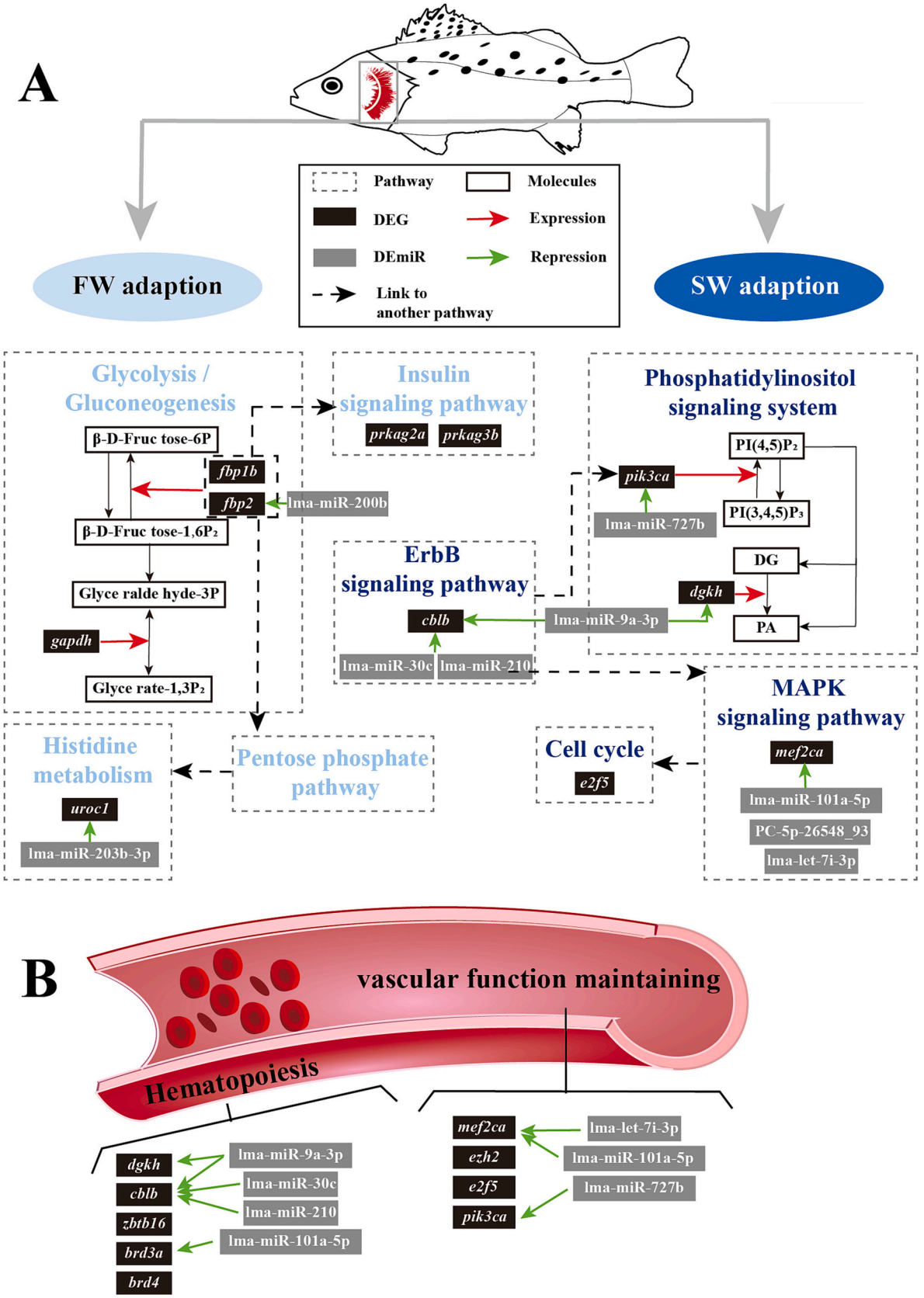

Fig. 8. Schematic diagram of predicted molecular mechanism during salinity acclimation in gills of spotted sea bass. A. key DEmiR, DEGs and pathways engaged in gills of spotted sea bass during FW and SW adaption. Key related pathways involved in FW and SW acclimation were marked in wathet and dark blue, respectively. B. Hematopoiesis associated key DEGs and DEmiRs involved in SW acclimation. The full names of genes were listed in Table S7. (For interpretation of the references to colour in this figure legend, the reader is referred to the web version of this article.)

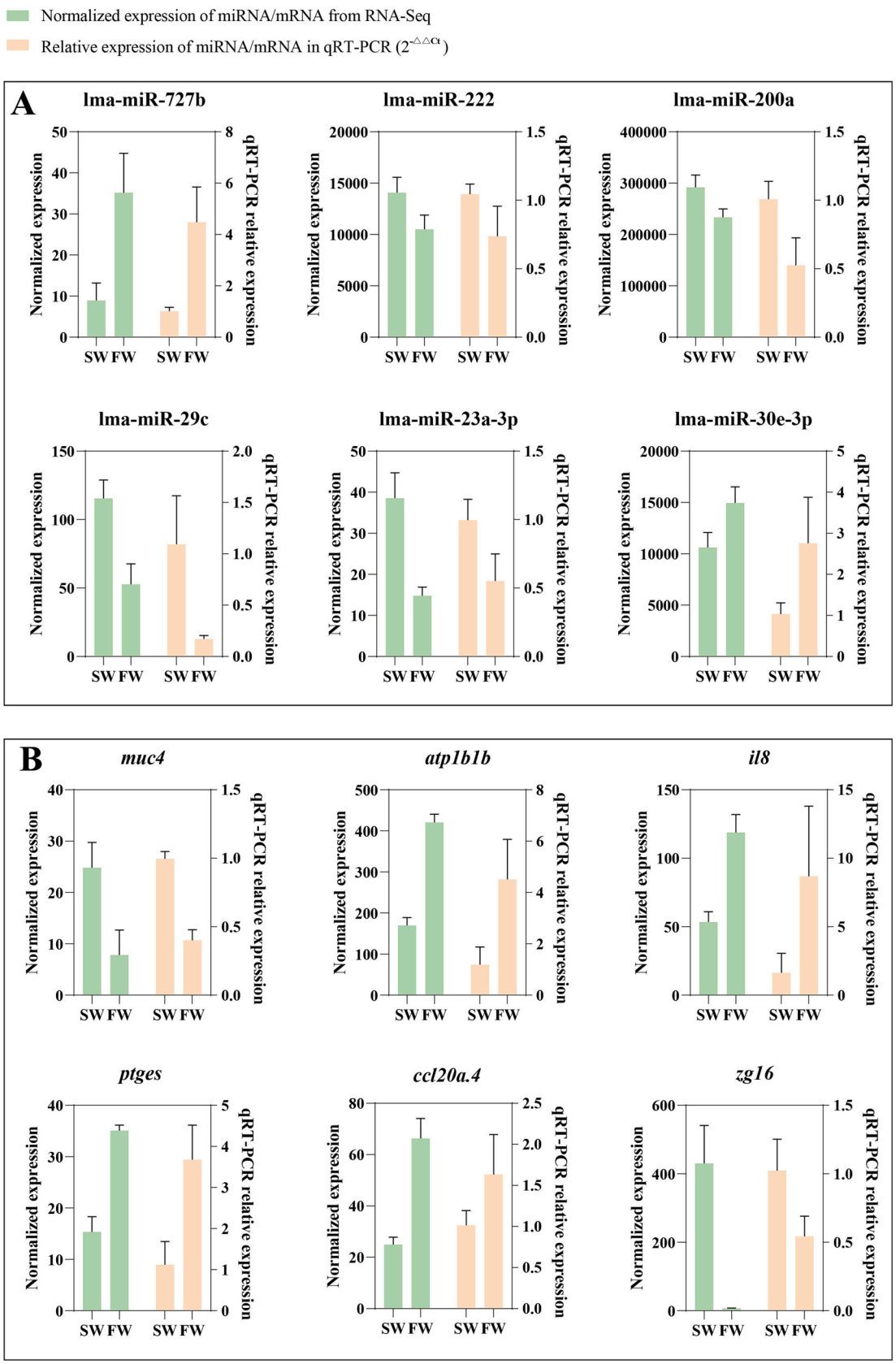

Fig. 9. qPCR validation in the gill of spotted sea bass. A. qPCR validation of 6 DEmiRs after FW and SW acclimation. B. qPCR validation of 6 DEGs after FW and SW adaption. The expression levels of the selected miRNAs and genes were normalized by U6 and 18S rRNA, respectively. Normalized expression values of miRNA/mRNA from RNA-Seq were filled with green, and relative expression levels of miRNA/mRNA generated by qPCR were shown in orange. (For interpretation of the references to colour in this figure legend, the reader is referred to the web version of this article.)

and hormones (Olson, 2002; Nilsson and Sundin, 1998). In our histological results, the number of red blood cells in gills of FW individuals was significantly lower than that of SW acclimated spotted sea bass. Similarly, in olive flounders (*Paralichthys olivaceus*), hematocrit and hemoglobin were significantly decreased at low salinity (Kim et al., 2021). Although the molecular mechanism of this phenomenon was poorly understood, we could deduce from our results that a number of hub genes in Cluster III and associated DEmiRs were reported as directly or indirectly related to the vascular events (Fig. 8B). For instances, hub genes like *brd3a*, *bra4* and *zbtb16* have been proved as essential hematopoiesis factors in zebrafish (Bielczyk-Maczynska et al., 2014; Poplineau et al., 2019). As a result, the down-regulation of lma-miR-101a-5p in SW acclimated spotted sea bass may increase the expression of *brd3a* to engage in osmotic regulation through hematopoiesis events (Fig. 8). Moreover, other hub genes including *ezh2*, *pik3ca* and *e2f5* were reported as vascular function maintenance molecules through promoting vascular development, maintaining vascular integrity, promoting the proliferation and migration of vascular smooth muscle cells (Li et al., 2018; Hare et al., 2015; Xu et al., 2019). Therefore, in our results, the decreased expression of lma-miR-727b after SW acclimation may induce the high expression of *pik3ca* to promote the change of vascular structure. Overall, the vascular networks identified within the gill ultimately link with gill functions, which further confirm the significance of the gill vascular system in osmotic regulation. In addition, molecules associated with tight junctions (TJs), which are intercellular junctions critical for building the epithelial barrier and maintaining epithelial polarity (Otani and Furuse, 2020), were concentrated in both FW and SW groups, and the enrichment of this category maybe correlated with the significant changes in the gill morphology and position of ionocytes during salinity acclimation process (Fig. 1).

5. Conclusions

In this study, we identified several key genes and miRNAs, as well as miRNA-mRNA regulation pairs that involved in salinity acclimation in gills of spotted sea bass, and hypothesized that glucose metabolism, signal transduction and the vascular system were crucial for osmotic regulation. Our findings will lay an essential foundation for elucidating the molecular mechanisms of salinity acclimation in gills, and we have identified a number of potential molecular markers that can be used for distinguishing seawater- and freshwater-cultured spotted sea bass. Moreover, this study provides a useful reference for potential future usage to improve the salinity tolerance capabilities and generate salinity-tolerance strains of stenohaline fish.

Funding

This work was supported by the National Natural Science Foundation of China [NSFC, grant number 32072947], and China Agriculture Research System [CARS, grant number CARS-47].

CRediT authorship contribution statement

Lingyu Wang: Conceptualization, Data curation, Formal analysis, Software, Methodology, Visualization, Writing – original draft, Writing – review & editing. **Xiaoyan Zhang:** Methodology, Investigation. **Haishen Wen:** Funding acquisition, Project administration, Resources. **Xin Qi:** Methodology, Resources. **Donglei Sun:** Methodology, Software. **Xueqi Li:** Data curation, Methodology. **Jinku Li:** Data curation, Methodology. **Yuan Tian:** Methodology. **Kaiqiang Zhang:** Methodology. **Yun Li:** Conceptualization, Validation, Supervision, Funding acquisition, Project administration, Resources, Writing – review & editing.

Declaration of Competing Interest

The authors declare that they have no known competing financial interests or personal relationships that could have appeared to influence the work reported in this paper.

Data availability

Data will be made available on request.

Appendix A. Supplementary data

Supplementary data to this article can be found online at https://doi.org/10.1016/j.aquaculture.2023.739778.

References

Abou, Anni I.S., Bianchini, A., Barcarolli, I.F., Varela, A.S., Robaldo, R.B., Tesser, M.B., Sampaio, L.A., 2016. Salinity influence on growth osmoregulation and energy turnover in juvenile pompano *Trachinotus marginatus* Cuvier 1832. Aquaculture. 455, 63–72. https://doi.org/10.1016/j.aquaculture.2016.01.010.

Aragao, C., Costas, B., Vargas-Chacoff, L., Ruiz-Jarabo, I., Dinis, M.T., Mancera, J.M., Conceicao, L.E., 2010. Mancera, L.E. Conceicao, changes in plasma amino acid levels in a euryhaline fish exposed to different environmental salinities. Amino Acids 38, 311–317. https://doi.org/10.1007/s00726-009-0252-9.

Bielczyk-Maczynska, E., Serbanovic-Canic, J., Ferreira, L., Soranzo, N., Stemple, D.L., Ouwehand, W.H., Cvejic, A., 2014. A loss of function screen of identified genome-wide association study loci reveals new genes controlling hematopoiesis. PLoS Genet. 10, e1004450 https://doi.org/10.1371/journal.pgen.1004450.

Cao, Q., Wang, H., Fan, C., Sun, Y., Li, J., Cheng, J., Chu, P., Yin, S., 2021. Environmental salinity influences the branchial expression of TCR pathway related genes based on transcriptome of a catadromous fish. Comp. Biochem. Physiol. Part. D. Genomics. Proteomics. 38, 100815 https://doi.org/10.1016/j.cbd.2021.100815.

Chaves Hernández, A.J., 2014. Poultry and avian diseases. In: Encyclopedia of Agriculture and Food Systems, pp. 504–520. https://doi.org/10.1016/B978-0-444-52512-3.00183-2.

Chen, X., Gong, H., Chi, H., Xu, B., Zheng, Z., Bai, Y., 2021. Gill transcriptome analysis revealed the difference in gene expression between freshwater and seawater acclimated guppy (*Poecilia reticulata*). Mar. Biotechnol. (NY). 23, 615–627. https://doi.org/10.1007/s10126-021-10053-4.

Douros, J.D., Baltzegar, D.A., Reading, B.J., Seale, A.P., Lerner, D.T., Grau, E.G., Borski, R.J., 2018. Leptin stimulates cellular glycolysis through a *stat3* dependent mechanism in tilapia. Front. Endocrinol. Lausanne 9, 465. https://doi.org/10.3389/fendo.2018.00465.

Edwards, S.L., Marshall, W.S., 2012. Principles and patterns of osmoregulation and euryhalinity in fishes. Fish. Physiol. 32, 1–44. https://doi.org/10.1016/B978-0-12-396951-4.00001-3.

Evans, T.G., Kultz, D., 2020. The cellular stress response in fish exposed to salinity fluctuations. J. Exp. Zool. A. Ecol. Integr. Physiol. 333, 421–435. https://doi.org/10.1002/jez.2350.

Flynt, A.S., Thatcher, E.J., Burkewitz, K., Li, N., Liu, Y., Patton, J.G., 2009. miR-8 microRNAs regulate the response to osmotic stress in zebrafish embryos. J. Cell Biol. 185, 115–127. https://doi.org/10.1083/jcb.200807026.

Gibbons, T.C., McBryan, T.L., Schulte, P.M., 2018. Interactive effects of salinity and temperature acclimation on gill morphology and gene expression in threespine stickleback. Comp. Biochem. Physiol. A. Mol. Integr. Physiol. 221, 55–62. https://doi.org/10.1016/j.cbpa.2018.03.013.

Hare, L.M., Schwarz, Q., Wiszniak, S., Gurung, R., Montgomery, K.G., Mitchell, C.A., Phillips, W.A., 2015. Heterozygous expression of the oncogenic Pik3ca(H1047R) mutation during murine development results in fatal embryonic and extraembryonic defects. Dev. Biol. 404, 14–26. https://doi.org/10.1016/j.ydbio.2015.04.022.

Jiang, J.L., Xu, J., Ye, L., Sun, M.L., Jiang, Z.Q., Mao, M.G., 2020. Identification of differentially expressed genes in gills of tiger puffer (*Takifugu rubripes*) in response to low-salinity stress. Comp. Biochem. Physiol. B Biochem. Mol. Biol. 243-244, 110437 https://doi.org/10.1016/j.cbpb.2020.110437.

Kim, J.H., Jeong, E.H., Jeon, Y.H., Kim, S.K., Hur, Y.B., 2021. Salinity-mediated changes in hematological parameters, stress, antioxidant responses, and acetylcholinesterase of juvenile olive flounders (*Paralichthys olivaceus*). Environ. Toxicol. Pharmacol. 83, 103597 https://doi.org/10.1016/j.etap.2021.103597.

Kultz, D., 2015. Physiological mechanisms used by fish to cope with salinity stress. J. Exp. Biol. 218, 1907–1914. https://doi.org/10.1242/jeb.118695.

Lai, K.P., Li, J.W., Wang, S.Y., Chiu, J.M., Tse, A., Lau, K., Lok, S., Au, D.W., Tse, W.K., Wong, C.K., Chan, T.F., Kong, R.Y., Wu, R.S., 2015. Tissue-specific transcriptome assemblies of the marine medaka *Oryzias melastigma* and comparative analysis with the freshwater medaka *Oryzias latipes*. BMC Genomics 16, 135. https://doi.org/10.1186/s12864-015-1325-7.

Li, X., Shahid, M.Q., Wu, J., Wang, L., Liu, X., Lu, Y., 2016. Comparative small RNA analysis of pollen development in autotetraploid and diploid Rice. Int. J. Mol. Sci. 17, 499. https://doi.org/10.3390/ijms17040499.

Li, R., Yi, X., Wei, X., Huo, B., Guo, X., Cheng, C., Fang, Z.M., Wang, J., Feng, X., Zheng, P., Su, Y.S., Masau, J.F., Zhu, X.H., Jiang, D.S., 2018. EZH2 inhibits autophagic cell death of aortic vascular smooth muscle cells to affect aortic dissection. Cell Death Dis. 9, 180. https://doi.org/10.1038/s41419-017-0213-2.

Liang, P., Saqib, H.S.A., Lin, Z., Zheng, R., Qiu, Y., Xie, Y., Ma, D., Shen, Y., 2021. RNA-seq analyses of marine medaka (*Oryzias melastigma*) reveals salinity responsive

transcriptomes in the gills and livers. Aquat. Toxicol. 240, 105970 https://doi.org/10.1016/j.aquatox.2021.105970.
Lin, C.H., Yeh, P.L., Lee, T.H., 2021. Time-course changes in the regulation of ions and amino acids in the hard clam *Meretrix lusoria* upon lower salinity challenge. J. Exp. Zool. A. Ecol. Integr. Physiol. 335, 602–613. https://doi.org/10.1002/jez.2503.
Lisboa, V., Barcarolli, I.F., Sampaio, L.A., Bianchini, A., 2015. Effect of salinity on survival growth and biochemical parameters in juvenile *Lebranchmullet Mugilliza* (Perciformes:Mugilidae). Neotrop. Ichthyol. 13, 447–452. https://doi.org/10.1590/1982-0224-20140122.
Liu, Y., Wang, H., Wen, H., Shi, Y., Zhang, M., Qi, X., Zhang, K., Gong, Q., Li, J., He, F., Hu, Y., Li, Y., 2020. First high-density linkage map and QTL fine mapping for growth-related traits of spotted sea bass (*Lateolabrax maculatus*). Mar. Biotechnol. (NY). 22, 526–538. https://doi.org/10.1007/s10126-020-09973-4.
Martin-Gomez, L., Villalba, A., Kerkhoven, R.H., Abollo, E., 2014. Role of microRNAs in the immunity process of the flat oyster *Ostrea edulis* against bonamiosis. Infect. Genet. Evol. 27, 40–50. https://doi.org/10.1016/j.meegid.2014.06.026.
Monroe, I., Wentworth, S., Thede, K., Aravindabose, V., Garvin, J., Packer, R.K., 2019. Activity changes in gill ion transporter enzymes in response to salinity and temperature in fathead minnows (*Pimephales promelas*). Comp. Biochem. Physiol. A. Mol. Integr. Physiol. 228, 29–34. https://doi.org/10.1016/j.cbpa.2018.10.018.
Nicholls, C., Li, H., Liu, J.P., 2012. GAPDH: a common enzyme with uncommon functions. Clin. Exp. Pharmacol. Physiol. 39, 674–679. https://doi.org/10.1111/j.1440-1681.2011.05599.x.
Nilsen, T.W., 2007. Mechanisms of microRNA-mediated gene regulation in animal cells. Trends Genet. 23, 243–249. https://doi.org/10.1016/j.tig.2007.02.011.
Nilsson, S., Sundin, L., 1998. Gill blood flow control. Comp. Biochem. Physiol. A. Mol. Integr. Physiol. 119, 137–147. https://doi.org/10.1016/s1095-6433(97)00397-8.
Obernosterer, G., Leuschner, P.J., Alenius, M., Martinez, J., 2006. Post-transcriptional regulation of microRNA expression. RNA 12, 1161–1167. https://doi.org/10.1261/rna.2322506.
Olson, K.R., 2002. Vascular anatomy of the fish gill. J. Exp. Zool. 293, 214–231. https://doi.org/10.1002/jez.10131.
Otani, T., Furuse, M., 2020. Tight junction structure and function revisited: (trends in cell biology 30, 805-817, 2020). Trends Cell Biol. 30, 1014. https://doi.org/10.1016/j.tcb.2020.08.004.
Park, H.J., Jang, H.R., Park, S.Y., Kim, Y.B., Lee, H.Y., Choi, C.S., 2020. The essential role of fructose-1,6-bisphosphatase 2 enzyme in thermal homeostasis upon cold stress. Exp. Mol. Med. 52, 485–496. https://doi.org/10.1038/s12276-020-0402-4.
Pelis, R.M., McCormick, S.D., 2001. Effects of growth hormone and cortisol on Na(+)-K(+)-2Cl(−) cotransporter localization and abundance in the gills of Atlantic salmon. Gen. Comp. Endocrinol. 124, 134–143. https://doi.org/10.1006/gcen.2001.7703.
Poplineau, M., Vernerey, J., Platet, N., N'Guyen, L., Herault, L., Esposito, M., Saurin, A. J., Guilouf, C., Iwama, A., Duprez, E., 2019. PLZF limits enhancer activity during hematopoietic progenitor aging. Nucleic Acids Res. 47, 4509–4520. https://doi.org/10.1093/nar/gkz174.
Pu, M., Chen, J., Tao, Z., Miao, L., Qi, X., Wang, Y., Ren, J., 2019. Regulatory network of miRNA on its target: coordination between transcriptional and post-transcriptional regulation of gene expression. Cell. Mol. Life Sci. 76, 441–451. https://doi.org/10.1007/s00018-018-2940-7.
Rajas, F., Gautier-Stein, A., Mithieux, G., 2019. Glucose-6 phosphate, a central hub for liver carbohydrate metabolism. Metabolites. 9, 282. https://doi.org/10.3390/metabo9120282.
Ren, Y., Tian, Y., Mao, X., Wen, H., Qi, X., Li, J., Li, J., Li, Y., 2022. Acute hypoxia changes the gene expression profiles and alternative splicing landscape in gills of spotted sea bass (*Lateolabrax maculatus*). Front. Mar. Sci. 9, 1024218. https://doi.org/10.3389/fmars.2022.1024218.
Ricardo, F., Peter, L., 1987. Energy partitioning in fish: the Activityrelated cost of osmoregulation in a Euryhaline cichlid. J. Exp. Biol. 128, 63–85. https://doi.org/10.1242/jeb.128.1.63.
Root, L., Campo, A., MacNiven, L., Con, P., Cnaani, A., Kultz, D., 2021. Nonlinear effects of environmental salinity on the gill transcriptome versus proteome of Oreochromis niloticus modulate epithelial cell turnover. Genomics. 113, 3235–3249. https://doi.org/10.1016/j.ygeno.2021.07.016.
Sabaliauskas, N.A., Foutz, C.A., Mest, J.R., Budgeon, L.R., Sidor, A.T., Gershenson, J.A., Joshi, S.B., Cheng, K.C., 2006. High-throughput zebrafish histology. Methods. 39, 246–254. https://doi.org/10.1016/j.ymeth.2006.03.001.
Shinji, J., Okutsu, T., Jayasankar, V., Jasmani, S., Wilder, M.N., 2012. Metabolism of amino acids during hyposmotic adaptation in the whiteleg shrimp, *Litopenaeus vannamei*. Amino Acids 43, 1945–1954. https://doi.org/10.1007/s00726-012-1266-2.
Shwe, A., Østbye, T.K., Krasnov, A., Ramberg, S., Andreassen, R., 2020. Characterization of differentially expressed miRNAs and their predicted target transcripts during smoltification and adaptation to seawater in head kidney of Atlantic salmon. Genes (Basel) 11, 1059. https://doi.org/10.3390/genes11091059.
Sternisha, S.M., Miller, B.G., 2019. Molecular and cellular regulation of human glucokinase. Arch. Biochem. Biophys. 663, 199–213. https://doi.org/10.1016/j.abb.2019.01.011.
Sun, Z., Lou, F., Zhang, Y., Song, N., 2020. Gill transcriptome sequencing and de novo annotation of *Acanthogobius ommaturus* in response to salinity stress. Genes (Basel) 11, 631. https://doi.org/10.3390/genes11060631.
Tian, Y., Shang, Y., Guo, R., Chang, Y., Jiang, Y., 2019. Salinity stress-induced differentially expressed miRNAs and target genes in sea cucumbers *Apostichopus japonicus*. Cell Stress Chaperones 24, 719–733. https://doi.org/10.1007/s12192-019-00996-y.
Tian, Y., Wen, H., Qi, X., Zhang, X., Sun, Y., Li, J., He, F., Zhang, M., Zhang, K., Yang, W., Huang, Z., Ren, Y., Li, Y., 2020. Alternative splicing (AS) mechanism plays important roles in response to different salinity environments in spotted sea bass. Int. J. Biol. Macromol. 155, 50–60. https://doi.org/10.1016/j.ijbiomac.2020.03.178.
Wienholds, E., Plasterk, R.H., 2005. MicroRNA function in animal development. FEBS Lett. 579, 5911–5922. https://doi.org/10.1016/j.febslet.2005.07.070.
Wienholds, E., Kloosterman, W.P., Miska, E., Alvarez-Saavedra, E., Berezikov, E., de Bruijn, E., Horvitz, H.R., Kauppinen, S., Plasterk, R.H., 2005. MicroRNA expression in zebrafish embryonic development. Science. 309, 310–311. https://doi.org/10.1126/science.1114519.
Wu, Q., Lu, R.L., Li, J.X., Rong, L.J., 2017. MiR-200a and miR-200b target PTEN to regulate the endometrial cancer cell growth in vitro. Asian Pac J Trop Med 10, 498–502. https://doi.org/10.1016/j.apjtm.2017.05.007.
Xiao, J., Zhong, H., Zhou, Y., Yu, F., Gao, Y., Luo, Y., Tang, Z., Guo, Z., Guo, E., Gan, X., Zhang, M., Zhang, Y., 2014. Identification and characterization of microRNAs in ovary and testis of Nile tilapia (*Oreochromis niloticus*) by using solexa sequencing technology. PLoS One 9, e86821. https://doi.org/10.1371/journal.pone.0086821.
Xu, Q., Liang, Y., Liu, X., Zhang, C., Liu, X., Li, H., Liang, J., Yang, G., Ge, Z., 2019. miR-132 inhibits high glucose-induced vascular smooth muscle cell proliferation and migration by targeting E2F5. Mol. Med. Rep. 20, 2012–2020. https://doi.org/10.3892/mmr.2019.10380.
Yan, B., Zhao, L.H., Guo, J.T., Zhao, J.L., 2012a. miR-429 regulation of osmotic stress transcription factor 1 (OSTF1) in tilapia during osmotic stress. Biochem. Biophys. Res. Commun. 426, 294–298. https://doi.org/10.1016/j.bbrc.2012.08.029.
Yan, B., Guo, J.T., Zhao, L.H., Zhao, J.L., 2012b. MiR-30c: a novel regulator of salt tolerance in tilapia. Biochem. Biophys. Res. Commun. 425, 315–320. https://doi.org/10.1016/j.bbrc.2012.07.088.
Yan, B., Zhu, C.D., Guo, J.T., Zhao, L.H., Zhao, J.L., 2013. miR-206 regulates the growth of the teleost tilapia (*Oreochromis niloticus*) through the modulation of IGF-1 gene expression. J. Exp. Biol. 216, 1265–1269. https://doi.org/10.1242/jeb.079590.
Yang, H., Cho, M.E., Li, T.W., Peng, H., Ko, K.S., Mato, J.M., Lu, S.C., 2013. MicroRNAs regulate methionine adenosyltransferase 1A expression in hepatocellular carcinoma. J. Clin. Invest. 123, 285–298. https://doi.org/10.1172/JCI63861.
Yang, W.K., Chung, C.H., Cheng, H.C., Tang, C.H., Lee, T.H., 2016. Different expression patterns of renal Na^+/K^+-ATPase α-isoform-like proteins between tilapia and milkfish following salinity challenges. Comp. Biochem. Physiol. B Biochem. Mol. Biol. 202, 23–30. https://doi.org/10.1016/j.cbpb.2016.07.008.
Yang, C., Zhou, Q., Ma, Q., Wang, L., Yang, Y., Chen, G., 2022. Differentially expressed miRNAs and mRNAs in regenerated scales of rainbow trout (*Oncorhynchus mykiss*) under salinity acclimation. Animals (Basel). 12, 1265. https://doi.org/10.3390/ani12101265.
Zhang, S., Zhao, F., Wei, C., Sheng, X., Ren, H., Xu, L., Lu, J., Liu, J., Zhang, L., Du, L., 2013. Identification and characterization of the miRNA transcriptome of Ovis aries. PLoS One 8, e58905. https://doi.org/10.1371/journal.pone.0058905.
Zhang, X., Wen, H., Wang, H., Ren, Y., Zhao, J., Li, Y., 2017. RNA-Seq analysis of salinity stress-responsive transcriptome in the liver of spotted sea bass (*Lateolabrax maculatus*). PLoS One 12, e0173238. https://doi.org/10.1371/journal.pone.0173238.
Zhang, H., Wu, J., Wu, J., Fan, Q., Zhou, J., Wu, J., Liu, S., Zang, J., Ye, J., Xiao, M., Tian, T., Gao, J., 2019. Exosome-mediated targeted delivery of miR-210 for angiogenic therapy after cerebral ischemia in mice. J. Nanobiotechnology. 17, 29. https://doi.org/10.1186/s12951-019-0461-7.
Zhang, Y., Wen, H., Liu, Y., Qi, X., Sun, D., Zhang, C., Zhang, K., Zhang, M., Li, J., Li, Y., 2022. Gill histological and transcriptomic analysis provides insights into the response of spotted sea bass (*Lateolabrax maculatus*) to alkalinity stress. Aquaculture. 563, 738945 https://doi.org/10.1016/j.aquaculture.2022.738945.
Zhou, Q.L., Wang, L.Y., Zhao, X.L., Yang, Y.S., Ma, Q., Chen, G., 2022. Effects of salinity acclimation on histological characteristics and miRNA expression profiles of scales in juvenile rainbow trout (*Oncorhynchus mykiss*). BMC Genomics 23, 300. https://doi.org/10.1186/s12864-022-08531-7.